Scientific Research Publishing

Journal of Biosciences and Medicines, 2022, 10, 13-33
https://www.scirp.org/journal/jbm
ISSN Online: 2327-509X
ISSN Print: 2327-5081

Development of a Targeted Drug Delivery System for the Treatment of SARS-CoV-2

Sahil Sood

Lambert High School, Duluth, United States of America
Email: sahilsood2005@gmail.com

How to cite this paper: Sood, S. (2022) Development of a Targeted Drug Delivery System for the Treatment of SARS-CoV-2. *Journal of Biosciences and Medicines*, **10**, 13-33.
https://doi.org/10.4236/jbm.2022.1010002

Received: May 28, 2022
Accepted: October 7, 2022
Published: October 10, 2022

Abstract

SARS-CoV-2 has triggered a public health outbreak across the world, resulting in almost 5 million deaths as of January 2022. The arrival of vaccines has provided temporary relief, but these vaccines target the spike protein, which is highly prone to mutation, making it impossible to develop a long-term cure for the coronavirus. As such, there is an urgent need for site-specific inhibition of the virus in the respiratory tract, as well as targeting the internal proteins of the virus itself. Past literature has identified 3CLpro and PLpro as enzymes essential to the replication of the virus, as they assemble almost the entirety of the viral genome; as such, inhibiting the activity of these enzymes can stymie the spread of the virus. This project proposes the use of inhaled drug delivery to inhibit Covid-19 by synthesizing a formulation that can travel directly to the lungs via inhalation. In order to streamline synthesis, existing FDA-approved drugs were analyzed using computational docking software and in vitro assays for inhibitory activity against these two enzymes. High-performing drugs were then encapsulated in PLGA nanoparticles to synthesize a drug delivery system, which was tested and characterized *in vitro*. Furthermore, in an effort to improve this drug delivery system relative to other drug delivery systems, the use of enzyme nanomotors was explored as a way to increase the accuracy of delivery by using computational simulations that mimicked conditions in the human body to model the velocity and trajectory of the nanomotors.

Keywords

Covid-19, SARS-CoV-2, PLGA, Drug Delivery, Chemotaxis

1. Introduction

Severe acute respiratory syndrome coronavirus 2 or SARS-COV-2 is a virus that

causes the novel coronavirus, an infectious respiratory disease whose emerging outbreak has resulted in a global pandemic. This zoonotic virus can cause fever, cough, shortness of breath, dyspnea, pneumonia, kidney failure, and even death. As of January 2022, there are 292 million cases worldwide, and over 5 million deaths [1]. These numbers are unprecedented in comparison to the related SARS coronavirus (SARS-COV), which had around 8000 cases and 800 deaths [2]. SARS-COV-2 is an enveloped virus with a positive RNA genome, and it belongs to the *Coronaviridae* family of the order *Nidovirales*. The virus is transmitted through droplets of water in the air being inhaled and entering the human body through the lungs, and it has four basic structures: the spike protein, envelope protein, membrane protein, and nucleocapsid protein. Virus surface spike proteins mediate the entry of SARS-COV-2 into human cells by enabling the circus to bind to the receptor protein hACE2 through its receptor-binding domain. From there, the viruses subsequently enter endosomes, and eventually fuse into viral and lysosomal membranes [2]. While vaccines have been developed, these vaccines do not prevent the transmission and spread of Covid-19, they simply mitigate its effects in some patients, meaning patients can still contract Covid-19 and potentially have fatal effects [3]. As such, the need for a drug delivery system that inhibits the spread of Covid-19 is necessary in order to secure public health, jumpstart the economy, and save millions of lives. Current drug treatments include broad-spectrum antiviral drugs, antimalarial drugs, anti-HIV infection drugs, and others, but the lack of site-specific target inhibition makes these drugs less specific in inhibiting the virus, thus decreasing their effectiveness.

Once inside the body, coronaviruses use important cysteine proteases in order to facilitate viral replication, enabling further severity of infection within the host, as well as the spread of infection to other host organisms. In SARS-COV-2, existing literature has determined two non-structural proteases that process polypeptides that are translated from the viral genome and create the necessary functional proteins to enable viral replication: 3-chymotrypsin-like protease (3CLpro) and viral papain like protease (PLpro) [4]. Thus, inhibition of these enzymes may hold the key to stymie the spread of the virus by preventing its replication within host organisms. As such, the identification of therapeutics to inhibit the activity of these two enzymes was crucial towards development of a targeted drug delivery system. Rather than develop entirely new polymers or compounds for viral inhibition, existing FDA-approved molecules were sought and the catalytic activity of the proteases in the presence of those molecules was tested in order to repurpose existing medications. This streamlines the process of creating a finalized drug delivery system for the treatment of Covid-19, as clinical trials and FDA approval are no longer required, which can often add months or even years to the time of development. Considering the urgency at which this formulation is required, especially with the recent resurgence of the virus with the Omicron variant, it is imperative that such a formulation be released to the public as rapidly as possible.

1.1. Drug Delivery Background

Drug delivery systems are systems that are designed to transport a drug or compound inside of a vesicle to the delivery site. These targeted systems are uniquely preferable to standard practices of taking medication (injection, oral consumption, etc.) because pharmacokinetics dictate that when taken in a standard manner, the drug is distributed throughout the entire body rather than one area. When treating viruses like Covid-19, which are confined to one area of the body (in this case, the respiratory tract), this results in only a fraction of the dosage taken reaching the area of interest, which lowers efficacy of the treatment. Oftentimes, this method of delivery utilizes nanomedicine, which employs nanoparticles as a vesicle to transport drugs to the site of interest, ultimately reducing the number of doses taken, reducing side effects, and increasing efficacy of the treatment [5].

Poly (lactic-co-glycolic acid), or PLGA, is a polymeric nanoparticle that has been well characterized in existing literature, and it is widely regarded as one of the most effective vesicles for drug delivery based on its sustained-release properties, low toxicity in the body, and biocompatibility with tissues and cells. PLGA is a copolymer of Poly (lactic acid) and Poly (glycolic acid), and it has the ability to carry a wide range of drugs and compounds, ranging from immunomodulators to anticancer agents. Specifically, a property of PLGA allows it to co-deliver several compounds simultaneously, which makes it uniquely fitting for this specific project, as two different compounds will likely be in the final formulation (one to inhibit 3CLpro and one to inhibit PLpro). Furthermore, PLGA has the ability to be dried into a powder for drug delivery via inhalation, enabling pulmonary drug delivery which can prove useful for respiratory conditions such as Covid-19. Its high mechanical strength ensures that the polymer does not break down easily in the body; it has a half-life of approximately 50 days, and it breaks down into benign compounds that do not interfere with bodily functions. Finally, PLGA is comparatively cost-effective in comparison to other nanoparticles (gold, silver, cobalt, etc). For instance, gold nanoparticles, which are often used in a myriad of projects, are $80 per mg, while PLGA is only $0.13 per mg. Since this research aims to develop a treatment that should be accessible to patients, materials with lower cost mean that more patients are able to access the benefits of the research. Finally, PLGA does not require a release mechanism, as the compound releases its contents over time as a sustained rate. Based on these properties, it was evident that PLGA would be an optimal vesicle to load the target drugs in for site-specific delivery by creating an inhaled formulation.

1.2. Enzyme Chemotaxis

Enzyme chemotaxis is an enzymatic phenomenon that describes the movement of enzymes towards their substrates through favorable thermodynamic conditions. Specifically, enzymes exhibit the process of chemotaxis moving along a

substrate concentration gradient as they can diffuse and move towards regions of high substrate concentration. There are two types of chemotaxis, positive and negative chemotaxis. Positive chemotaxis entails the movement towards higher substrate concentrations, whereas negative chemotaxis is the movement away from higher substrate concentrations. Negative chemotaxis only exists in certain drug delivery systems due to Hofmeister salt interactions between lipid membranes and substrates. As such, creating a drug delivery system with a vesicle that is not composed of lipids (such as PLGA) means that the chemotaxis will only be positive.

The theory of enzyme chemotaxis pertains to how enzymes catalyze reactions with their substrates. Strong binding interactions between enzymes and substrates correlate to higher chemotactic velocity, but too strong binding interactions (*i.e.* irreversible binding) prevents chemotaxis from occurring, as the fraction of free enzymes goes to 0. It is important to note an enzyme with an occupied active site does not exhibit chemotaxis; only free enzymes chemotaxis. As such, the total chemotactic velocity is dependent on the fraction of free enzyme available, which is directly related to the concentration of substrate. As such, at higher concentrations of substrate, chemotaxis begins to slow as less enzymes are free to move towards higher substrate concentrations.

The use of chemotaxis is especially pertinent in the field of targeted drug delivery, as nanovehicles can be coated in an enzyme, and the attraction between that enzyme and its substrate can be used to propel nanovehicles closer to the therapeutic target, ensuring that the release of the drug is in close proximity to the target, thereby increasing the efficacy of the drug delivery system. Already, Somasundar *et al.* explored the use of certain chemotactic enzymes as nanomotors for drug delivery [6]. Similarly, this project aims to characterize the chemotaxis of enzymes relevant to targeted drug delivery for Covid-19 using Michaelis-Menten kinetics, one of the most widely-accepted models for enzyme kinetics. Furthermore, the enzyme's chemotaxis must overcome Brownian diffusion, which is the random motion of particles in a fluid medium resulting from collisions with surrounding molecules. Brownian diffusion is the main opposing force to chemotaxis once in the body, as in order for the nanovehicle to chemotax towards the target, it must outpace the particle's tendency to follow random motion patterns.

1.3. Status Quo Problems

Currently, there exist treatments for the novel coronavirus in the form of vaccines, produced by companies like Pfizer and Moderna. These mRNA vaccines utilize the spike protein, a membrane protein responsible for enabling the virus to enter human cells, as a means to stimulate production of antigens and antibodies in the body to help build immunity to the virus. However, there are two major issues with this method. The first is that these vaccines do not stop the spread of the virus; while there is a slight decrease in transmission rates, the virus mainly serves to mitigate the severity of the disease in the body. However,

this is not successful for all patients. Second, the virus targets the ever-mutating spike protein, which creates a moving target for pharmaceutical innovators. As the spike protein continues to mutate, new doses of the vaccines will have to be released in order to build immunity to that specific spike protein, which would overall be infeasible for large scale distribution and herd immunity. As such, there lies a need for specific inhibition of the core enzymes within the virus, like 3CLpro and PLpro, rather than the surface proteins that are subject to constant mutation. This ensures that a long term cure to these coronaviruses, as well as future coronaviruses, is developed, along with ending the pandemic by preventing transmission of the disease by inhibiting its ability to spread within the body.

1.4. Research Objectives

When analyzing the above circumstances, a project began to formulate with three main objectives:

First: the goal was to identify existing FDA-approved compounds that could be used to inhibit 3CLpro and PLpro. Seeing as the implications of this research exist in the present and the need for a treatment is imminent, the use of FDA-approved compounds enables this treatment to reach patients faster, as it bypasses any necessary approval steps from the FDA specifically. Not only does this ensure the compounds are safe to be used, but it also saves time and resources comparatively. This is because drug discovery/drug synthesis projects require substantially more time and more resources, which was not a luxury that could be afforded during the pandemic.

Second: the project aimed to synthesize nanoparticles for drug delivery with the identified compounds and test their efficacy *in vitro*, as nanomedicine is a viable method by which these drugs can be delivered directly to the lungs. Specifically, using PLGA as a vesicle appeared most prudent in the experimental design phase of the research, due to its aforementioned benefits.

Third: while this would be the only drug delivery system designed to treat SARS-COV-2, this drug delivery system was designed to be better than existing drug delivery systems with other diseases through the use of enzyme nanomotors. Upon the initial literature review and the discovery of the phenomenon of enzyme chemotaxis, it was evident that this interaction between the enzyme and its substrate could be easily utilized as a means to make a broader contribution to the field of drug delivery, as well as make this drug delivery system more accurate and precise, enabling better treatment for the millions afflicted with the virus.

1.5. Creation of a Drug Delivery System

With the above in mind, this project aims to develop an inhaled formulation for the treatment of Covid-19 by identifying potential drugs, synthesizing the nanoparticles to create a targeted drug delivery system, and characterizing its movement in the body. PLGA nanoparticles that are coated in a chemotactic enzyme would be loaded with compounds that inhibit 3CLpro and PLpro and

delivered to the body through the lungs, where the SARS-COV-2 virus mainly resides. The project was split into 3 distinct phases: screening and testing FDA approved drugs and phytochemicals to determine those with inhibitory activity of 3CLpro/Plpro, synthesizing PLGA nanoparticles with the drugs determined from the first phase, and computationally modeling the movement of those nanoparticles within the body. To identify potential inhibitors, 3987 FDA approved drugs and phytochemicals in the SuperDrugs2 database were computationally filtered based on their structure to determine potential drug candidates for the inhibition of 3CLpro and PLpro. 47 selected drugs were then tested in enzymatic inhibitor-screening assays in order to eliminate potential false positives. From there, the drugs that yielded the best results for enzymatic inhibition (stromectol had high inhibition of 3CLpro, and aloin has high inhibition of PLpro) were then loaded into PLGA nanoparticles and analyzed using a nanosizer, high performance liquid chromatography (HPLC), scanning electron microscope (SEM), and Fourier-transform infrared spectroscopy (FTIR). Finally, in order to model the motion of the nanoparticles, *in vitro* and *in vivo* testing had been planned; unfortunately, due to Covid-19 restrictions and new policies because of the Omicron variant, the lab became unavailable, so the motion of the particle was instead modeled *in silico*. As shown in the literature, beta actin, an actin isoform in humans that composes the cytoskeleton, is upregulated in the presence or SARS-COV-2, with a concentration gradient that increases with proximity to the virus. Furthermore, it has been shown that protein kinase C delta (PKC-delta) exhibits enzyme chemotaxis towards increasing concentrations of beta actin. Based on such, the Stokes-Einstein equation and Michaelis Menten kinetics were utilized to quantify the net chemotactic velocity of PKC-delta across the concentration gradient of beta actin. Furthermore, the Python library PyBroMo was used to characterize the Brownian diffusion of the particle in the body and determine whether chemotaxis can outpace Brownian diffusion.

2. Procedures

2.1. Identification of Inhibitors

The identification of potential inhibitors was carried out with the help of a lab group at the local medical school. 3987 FDA approved drugs from the SuperDrugs2 database were downloaded and sorted as viral protease inhibitors, viral non-protease inhibitors, and off-target drugs. The drugs were then docked with a monomeric form of 3CLpro using the Molecular Operating Environment (MOE) software. Binding affinities for the drugs were taken and used to rank the drugs, with −6.5 kcal/mol used as the cutoff S score. Drugs with a higher binding affinity were tested in an *in vitro* enzymatic assay to eliminate the potential for false positives and further understand the biological aspects. Using commercially available assay kits from BPS Biosciences, inhibitory activity of the drugs of 3CLpro and PLpro was measured, and it was experimentally determined that stromectol had the highest inhibition of 3CLpro, and aloin had the highest inhi-

bition of PLpro.

The procedure for the assays is as shown:

All reagents including enzymes are aliquoted and stored at −20 *degrees C and* −80 *degrees C. Keep on ice until thawed.*

1) Take out 1 well of enzymatic inhibitor and dithiothreitol (DTT). Keep on ice until thawed.

2) Take out the buffer and keep it at room temperature to thaw.

3) Put 3 mL of assay buffer in each petri dish. Add 6 microliters DTT and 1 vial of enzyme.

4) Add 30 microliters of enzyme assay buffer to all wells except blanks.

5) Add 30 microliters of assay buffer to **only** blanks.

6) Add 10 microliters of inhibitor to inhibitor control wells.

7) Add 10 microliters of 1% dimethyl sulfoxide (DMSO) solution to blank wells and negative control wells.

8) Add 10 microliters of 250 micromolars of drugs to the rest of the test wells.

9) Shake for approximately 30 seconds.

10) Incubate at room temperature for 30 - 40 minutes.

11) After incubation, add the respective substrate of the enzyme as prepared below:

a) 1 mL assay buffer;

b) 2 microliters DTT;

c) 1 aliquot of substrate.

12) Add 10 microliters of substrate mixture prepared above to all 96 wells.

13) Seal plate and ensure removal of all bubbles in the seal.

14) Shake briefly to mix the substrate.

15) Incubate overnight at room temperature

16) Read data at 360 by 460 nm using fluorescence on the plate reader.

Ultimately, there should be 4 distinct types of wells:

1) Negative Control Wells:

a) Enzyme;

b) Assay buffer;

c) Substrate;

d) DMSO.

2) Positive Control Wells:

a) Enzyme;

b) Assay buffer;

c) Inhibitors;

d) Substrate.

3) Blank Wells:

a) Assay Buffer;

b) DMSO;

c) Substrate.

4) Test Wells:

a) Enzyme;

b) Assay buffer;

c) Substrate;

d) Drug.

Plate Reader Operation:

1) Switch on the plate reader and open the plate reader application on connected desktop/computer;

2) Select standard protocol;

3) For procedure, select "shake 5 seconds";

4) For reading the data, select the fluorescence setting;

5) For the wavelength, check 360 × 460 nm and gain 50;

6) Confirm all parameters and start the reading process;

7) Save the data file as an excel file.

2.2. Synthesis of PLGA Nanoparticles

The synthesis of the nanoparticles was conducted independently under the supervision of a professor at a local medical school. In order to load PLGA nanoparticles with the target drug, the double emulsification method was used, for which the protocol is written below. For some formulations, the compound indocyanine green (ICG) was added in addition to the drug, as ICG acts as a fluorescent tag in the body. This enables better quantification of the release profile and tracking of the drug when *in vivo* studies are conducted in the future.

Nanoparticle Preparation:

All steps involving solvent or dissolved/emulsified polymer were performed in a chemical fume hood.

1) Weigh 100 mg (+/− 5 mg) of poly (lactic-co-glycolic acid) (PLGA), place in a 13 mm × 100 mm test tube, and dissolve is in 1 ml of dicholormethane (DCM) using a glass serological pipette.

2) Vortex the sample on high until all polymer is completely dissolved (approx. 10 min).

3) Add 45 ml of 0.3% w/v polyvinyl chloride (PVC) to a 200 ml glass beaker with a magnetic stir bar and set stirring speed to 360 rpm, and add 2 ml to a 13 mm × 100 mm test tube.

4) Add drug:

For *stromectol* (*hydrophobic*): add stromectol directly to the PLGA solution (being careful to avoid the walls of the test tube) and vortex the tube until the encapsulant is homogeneously dispersed

For *aloin* (*hydrophilic*): Add up to 50 µl of aloin in water to the surface of the polymer solution. Ultrasonicate solution briefly on ice to emulsify the drug with polymer (typically 10 sec, or as necessary to achieve a homogenous, opaque solution).

5) Place the open tube polymer/drug solution near a vortexer. While holding the test tube containing PVC vertically and on high vortex, use a glass Pasteur

pipette to add the polymer/drug solution dropwise. Be careful to avoid the sides of the tube and drop the polymer solution directly onto the surface of the vortexing emulsifier. After the entire polymer solution has been added to the PVC, vortex the emulsion for 15 sec (*emulsions shown below*).

6) Immediately transfer the emulsified polymer to the ultrasonicator. Keep the test tube immersed in ice water and sonicate the emulsion in three 10 sec bursts (40% amplitude for a 700 W sonicator, 1/8 in probe tip size). As shown in **Figure 1**, move the emulsion up and down the probe to ensure even sonication, being careful to avoid touching the probe to the sides or bottom of the test tube. Pause between each ten second sonication to allow the solution to cool before proceeding (*step shown below*).

7) Add 1 - 2 ml of 0.3% PVC from the stirring solution to the emulsion with a glass Pasteur pipette, which thins the emulsified polymer so that it will pour more easily. **Figure 2** shows what the solutions should look like. Empty the emulsion into the stirring solution.

8) Allow nanoparticles to harden while stirring for three hours (*stirring solutions shown below in* **Figure 3**).

Figure 1. Emulsified polymer being sonicated.

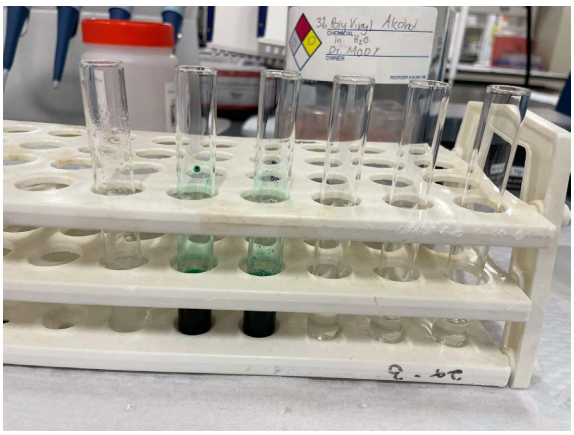

Figure 2. All emulsified polymers.

Figure 3. Stirring solutions under a fume hood.

Nanoparticle Collection:

1) Split the hardened nanoparticles into two centrifuge tubes (30 ml nominal volume) and balance to within 0.1 g.

2) Centrifuge nanoparticles in a fixed-angle rotor for 20 min at 20,000 RPM (*step shown below*).

3) Discard the supernatant, being careful not to disturb the nanoparticle pellet. Add 15 ml diH_2O and use a water bath sonicator to completely resuspend the nanoparticles.

4) Combine the contents of the two centrifuge tubes into one and repeat steps 2 and steps 3 2× more, for a total of three washes in 30 ml of diH_2O each time. The fluid volume of the last pellet resuspension should be 4 - 5 ml.

5) Separate a 1 ml aliquot of the sample for SEM imaging. Transfer the remaining sample to a preweighed 5 ml centrifuge tube and freeze at −80˚C for a minimum of 30 min.

6) Moving quickly so as not to let the frozen contents melt, uncap the tube and cover the top by securing lab tissue across the top with a rubber band. **If any melting occurs, refreeze before placing in the lyophilizer.

7) Lyophilize 72 hr for a 5 ml volume. Store lyophilized particles in Parafilm-wrapped tube at −80˚C (*step shown below*).

This protocol was used to develop 6 distinct formulations: PLGA Blank (as a control), PLGA-ICG (as a control), PLGA-stromectol, PLGA-stromectol-ICG, PLGA-Aloin, PLGA-Aloin-ICG.

HPLC Column Method:

For stromectol, the mobile phase consisted of methanol:acetonitrile: water

(45:50:5 v/v/v), with 0.2% acetic acid. The column was run for 20 minutes at a flow rate of 2 ml/min and detection was performed at 365 nm excitation and 475 nm emission. For aloin, the mobile phase consisted of different ratios of MilliQ water (A) and acetonitrile (B). The column was run for 24 minutes, with a gradient program of 80A: 20B at 0 min to 20A: 80B at 23 min, and then back to 80A: 20B at 24 min. The flow rate was 0.9 ml/min, and the detection was done at 254 nm. For both drugs, the injection volume was 50 microliters.

2.3. Chemotaxis Model

Michaelis-Menten:

The Michaelis-Menten model of enzyme kinetics is one of the oldest and most popular equations to describe the properties of enzymes. As Michaelis-Menten originally described the rate of enzyme reactions, new models have been developed that use this equation to describe the chemotaxis of enzymes by using their substrate-binding affinity, catalytic turnover, and level of diffusion enhancement in order to quantify the movement of a given enzyme along a gradient based on certain constants. This method is significantly more accurate than past models as it uses modifications to more accurately estimate the magnitude of the chemotaxis of free enzymes in a system.

In order to assess the viability of PKC-Delta as a nanomotor for drug delivery, a modified version of the Michaelis Menten equation was used to plot the net chemotactic velocity over an interval of beta actin concentration:

$$U_{chem}^{net} = D_E^0 \frac{K_m}{K_m + [S]} \frac{\partial_x}{K_d + [S]}$$

In order to derive this equation, we started with an existing equation in the literature, shown here:

$$U_{chem}^{E} = D_E^0 \frac{\partial_x [S]}{K_d + [S]}$$

This equation quantifies the chemotactic velocity if all free enzymes in the system were to chemotax. We multiplied this value by the rate of reaction, which quantifies the fraction of free enzymes that remain as substrate concentration increases. Ultimately, this resulted in the final equation for the net chemotactic velocity of the enzyme (U_{chem}^{net}). In this equation, D_E^0 represents the diffusivity of the enzyme in the absence of substrate. The variable K_m represents the Michaelis constant, which is the concentration of the substrate for a specific enzyme when the reaction rate for that enzyme is half of its maximum reaction rate. The term $[S]$ acts as the independent variable in this model, and it represents substrate concentration. The term $\partial_x [S]$ represents the concentration gradient of the substrate molecules, which can be calculated by dividing substrate concentration by the average capillary length in the body. Finally, the term K_d is the dissociation constant of the enzyme-substrate complex. By determining the values of these parameters for our specific system, we were able to

plot the net chemotactic velocity at different substrate concentrations.

The first term in this equation represents the diffusivity of the enzyme in the absence of substrate. In order to calculate the diffusivity of the enzyme, we used the Stokes-Einstein equation, shown here:

$$D = \frac{k_b T}{6\pi n r}$$

In this equation, which solves for the enzyme's diffusivity (D), k_b represents the Boltzmann constant, a widely known physical constant that equals 1.380649 $\times 10^{-23}$ joule per kelvin. T represents the temperature of the system, in Kelvin. In addition, n is the viscosity of the medium and r is the radius of the particle itself (in this case, the radius of the nanoparticle). The values of the parameters used were based on the human body, so the temperature was 310.15 K, viscosity was 0.004 Pascal-seconds, and the radius was 132 nm (experimentally determined from SEM), which yielded a diffusivity of 430249.08 nanometers squared per second.

For the following terms in the equation, the value of the Michaelis and dissociation constants of PKC-delta was needed, which were both found in the existing literature to be the same, at 36 micromolars [7]. Substrate concentration was the independent variable, and for the concentration gradient, the beta actin concentration divided by the average capillary length yielded a value of 25 micromolars per nanometer.

Brownian Motion:

The mean-squared displacement of particles can be calculated with the equation

$$\left\langle \vec{r}(t) - \vec{r}(t+\tau) \right\rangle = 2DN\tau$$

where $\vec{r}(t)$ is the position of the particle at the time defined by t, N is the number of dimensions being modeled, D is the diffusion coefficient of the particle, described by Michaelis-Menten kinetics as diffusivity, and τ is the interval of time being modeled. By utilizing this process alongside the coefficient D that was already calculated by the Stokes-Einstein equation above, a simulation was designed to determine Brownian motion.

The simulation was written in the programming language Python with the physics library PyBroMo. Using PKC-delta's parameters, 100 independent trajectories were introduced into the simulation and randomly sampled over 1000 time steps that each represented one second. By comparing the expected distance from the origin for each point with the actual distance from each point (finding the residual), the mean displacement per particle per second was found and then averaged across the simulation to the extent of the displacement induced by Brownian motion. Using the mean squared displacement equation, the theoretical displacement of each particle was also calculated and plotted. This value was then compared to the net chemotactic velocity in order to determine the viability of PKC-delta as a nanomotor for this drug delivery system.

3. Results/Discussion

3.1. Identification of Inhibitors

Computational analysis of drugs with the enzymes in the MOE yielded critical results regarding inhibition of the activity of 3CLpro and PLpro. In 3CLpro, Cys145, a critical amino acid in the active site of the enzyme, appeared to be the main amino acid that drugs with high binding affinity and high inhibition seemed to bind to. With stromectol specifically, the carbonyl group in its atomic structure binded to the side group on Cys145, which ultimately resulted in inactivity of the enzyme. This proved that Cys145 was an important amino acid to the function of the entire enzyme. Similarly, with Plpro, results showed Glu166, another amino acid in the active site, was the specific amino acid where most inhibitors would bind. With aloin, the hydroxyl groups in its structure binded to the side chains on Glu166, ultimately inhibiting the function of the enzyme. These results are critical for future research as more compounds are discovered that could potentially inhibit the activity of these enzymes.

Overall, 56 drugs passed the computational phase and were subsequently tested with the *in vitro* assays. Among them, 9 of the drugs were eliminated on face due to high autofluorescence in the drugs themselves, which would interfere with the fluorescence assays and make it difficult to obtain meaningful results. This left 47 drugs to be tested with the *in vitro* assays. Each drug was run in triplicates, meaning on each assay, there were 3 of the same well in order to confirm that the results across wells lined up. Furthermore, in order to remove the error between assays, a minimum of 5 assays was required to make any sound conclusion about the inhibition of a drug.

The experimental data in **Figure 4** shows that of the drugs screened for 3CLpro activity, stromectol has the most inhibition, making it the most optimal candidate when targeting 3CLpro. In fact, the data showed that stromectol has a half-maximal inhibitory concentration (IC_{50}) of only 21 micromolars, which is the concentration of stromectol needed to reduce 3CLpro activity by 50%. One of the limitations that may arise with the use of stromectol is the recent public backlash regarding stromectol's toxicity in the human body; however, stromectol is only toxic in high concentrations. Since this system is a targeted drug delivery system, all of the stromectol loaded will reach the lungs, whereas when taken regularly, only a fraction of the stromectol taken reaches the lungs to inhibit SARS-COV-2. Therefore, patients have to take substantially higher doses in order to get the same amount of stromectol to the lungs that this drug delivery system does, which can ultimately be toxic. Fortunately, the nature of this drug delivery system alleviates that concern and makes stromectol a safe therapeutic to use. For aloin, the data showed similar results, as there was almost complete inhibition of PLpro, and the IC_{50} value was 13.5 micromolars, indicating high levels of inhibition from both therapeutics. The IC_{50} values were calculated by conducting a nonlinear curve fit of the percent inhibition of the drug plotted against the log of the concentrations of the drug.

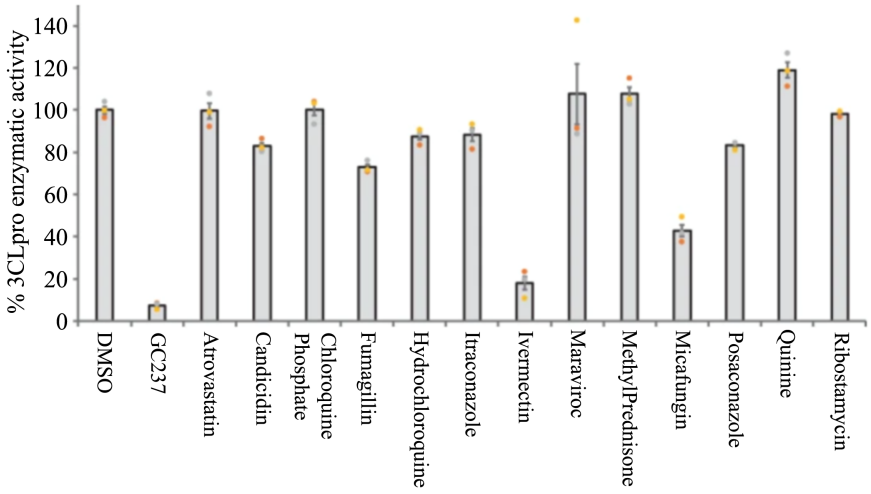

Figure 4. Enzymatic activity of drugs screened with assays.

3.2. Synthesis of PLGA Nanoparticles

When analyzing the results of the synthesis of the nanoparticles, two types of results were considered. The first were results that validated a successful synthesis, such as the use of Fourier Transform Infrared Spectroscopy (FTIR) or High-Performance Liquid Chromatography (HPLC) in order to confirm that the compounds were successfully encapsulated in the nanoparticles. The second type of results related to the nanoparticles themselves and their viability as a treatment, which assessed their toxicity in the body and their inhibitory abilities against their respective enzymes.

The FTIR spectra serve as confirmation of the experimental procedure. FTIR uses infrared radiation to bend and stretch the bonds by shining a low frequency light, and based on which frequency the sample absorbs at (which appears as lower transmittance on the spectra), that determines the functional groups present in the molecule. The lower the transmittance, the more of that functional group that is present, which can be used to confirm the loading of the drug, if the IR spectra line up with the molecular structure. The spectra all indicate that the experimental procedure was successful and stromectol/aloin were successfully emulsified within the PLGA nanoparticle. For instance, in **Figure 5(b)**, the spectra visibly shows a dip at approximately 3400 cm^{-1} that is not present in samples without aloin, which corresponds to the wavelength at which O-H (hydroxyl) groups stretch and absorb. This accurately reflects the structure of aloin, which has several hydroxyl groups. Similarly, in **Figure 5(a)**, there is a significant dip in transmittance at 1700 cm^{-1} that corresponds to carbonyl groups, indicating that the synthesis of the nanoparticles was correct.

The use of HPLC enables the creation of a calibration curve for both stromectol and aloin, providing a means to determine the concentration of either drug in a given sample of nanoparticles. Known concentrations of stromectol and aloin were analyzed at optimal wavelengths using HPLC, as depicted in **Figure 6**, and a calibration curve was built based on the data.

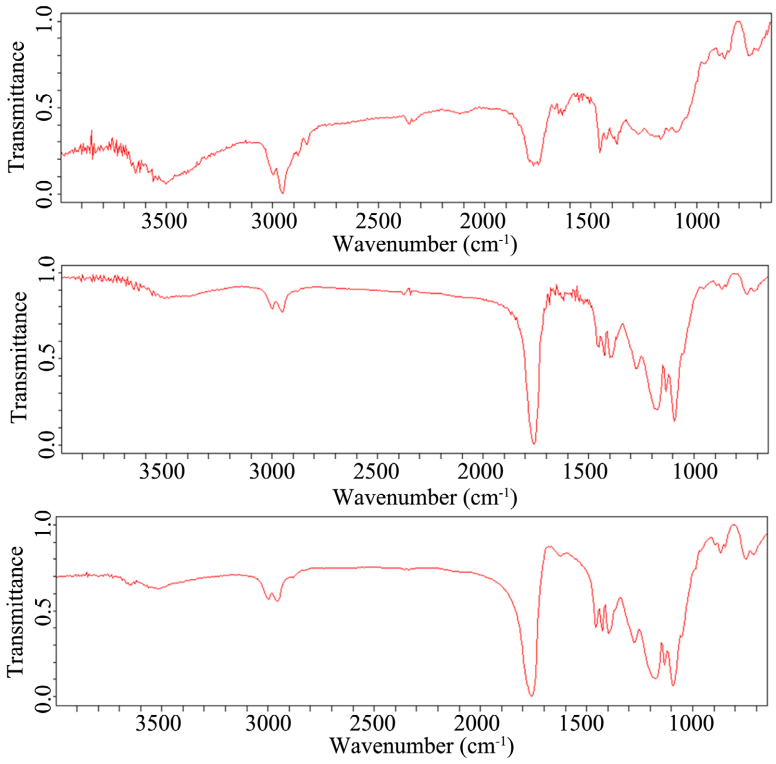

(a)

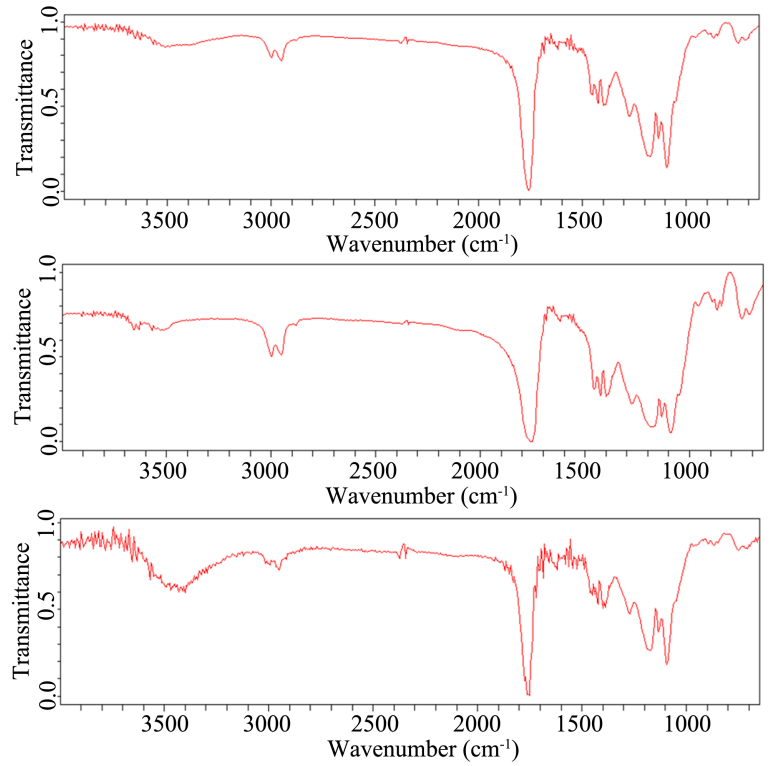

(b)

Figure 5. (a) and (b): FITR spectra for each formulation. (a) top to bottom: PLGA Blank, PLGA-ICG, PLGA-Stromectol. (b) top to bottom: PLGA-Stromectol-ICG, PLGA-Aloin, PLGA-Aloin-ICG.

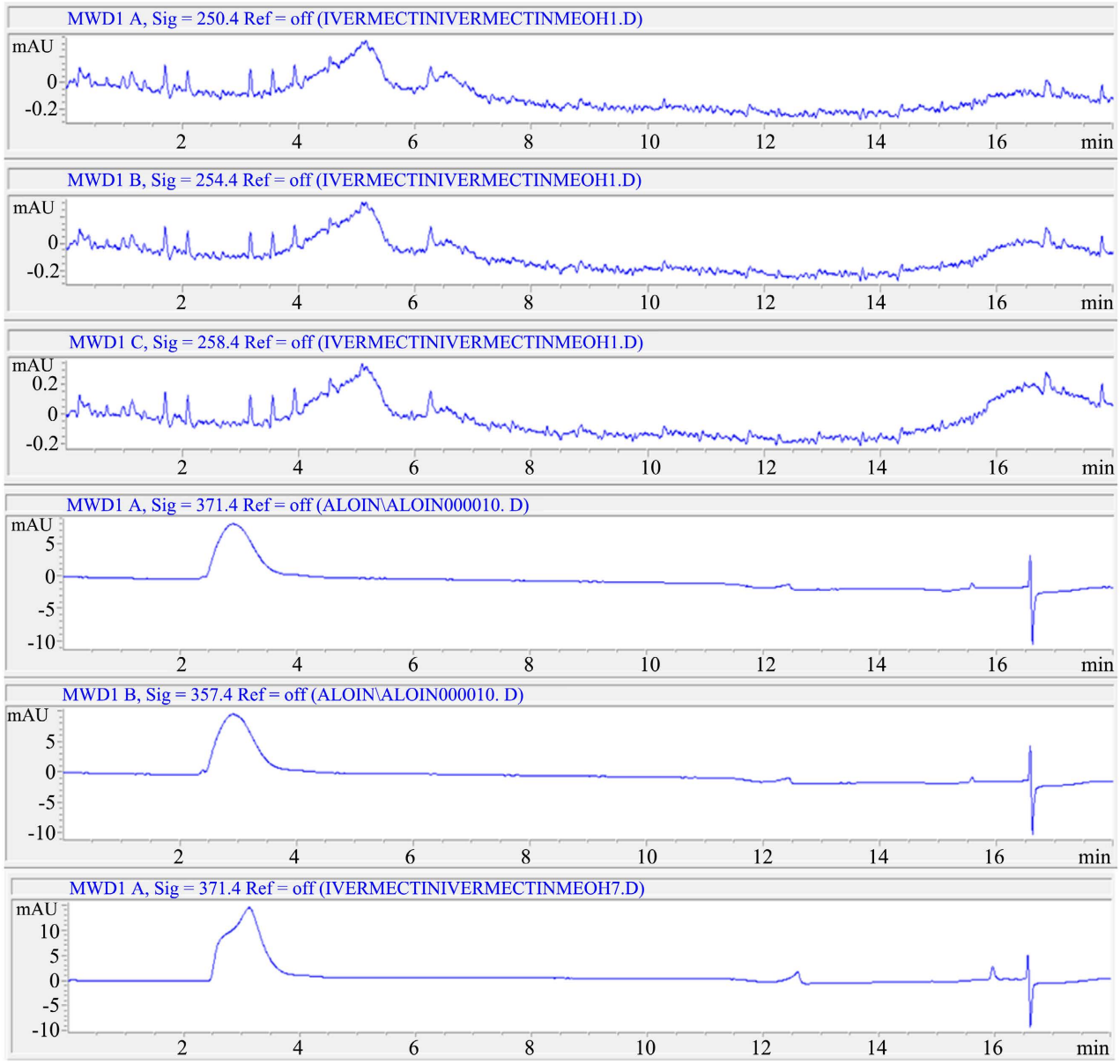

Figure 6. HPLC quantifications for known concentrations of stromectol (top 3) and aloin (bottom 3).

Using a Nanosizer, particle size measurements for each of the formulations were also taken, as shown in **Table 1**. The particle size is most directly related to the ability of the nanoparticles to successfully reach the target upon inhalation. The ideal size for these nanoparticles should be between 100 and 500 nm, as if it is smaller than 100 nm, it will be exhaled due to its low weight, and if it greater than 500 nm, the particle will get trapped in the mucus lining of the respiratory tract. Seeing as an enzyme coating would only add approximately 10 nm to the particle size, the particles are still an optimal size even with an enzyme coating.

The SEM images in **Figure 7** show that the particles are spherical in nature, which further validates that the experimental process was carried out correctly. This also confirms that when tested *in vivo*, these particles will be able to move

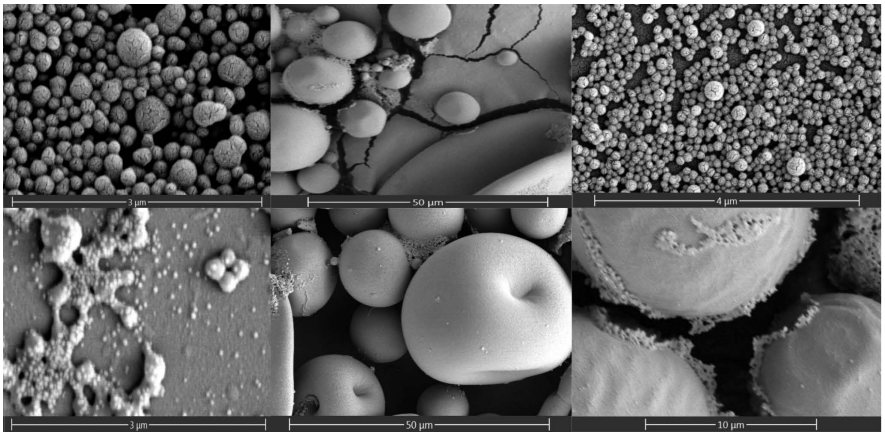

Figure 7. SEM images of each formulation. First row, left to right: PLGA, PLGA-ICG, PLGA-Stromectol. Second row, left to right: PLGA-Stromectol-ICG, PLGA-Aloin, PLGA-Aloin-ICG.

Table 1. Particle size of each formulation using Nanosizer.

Nanoparticle Formulations	Particle Size (nm)
PLGA Blank	100
PLGA-ICG	160
PLGA-STR	172
PLGA-STR-ICG	255
PLGA-Aloin	159
PLGA-Aloin-ICG	175

through the respiratory tract with ease and reach the virus in order to inhibit its activity. If the nanoparticles were rod or cone-shaped, that would indicate an incorrect procedure and decrease the efficacy of the drug delivery system, as it would mean less of the nanoparticles reach the site-specific target. The SEM images also confirm there are no structural surface flaws in the nanoparticle that could hamper its performance during testing. Finally, the spherical nature of these particles allows them to be properly represented by the subsequent Brownian diffusion model, as that model relies on the assumption that the particles are spherical in shape.

Finally, when these formulations were tested with *in vitro* assays, the results showed that the inhibition *in vitro* with the nanoparticles was approximately the same as the inhibition for the compound alone; around 84%, as shown Figure 8 above. The data tables are fluorescence readings taken from a plate reader of a well plate that tests 24 different drugs/formulations for activity against the enzymes. The upper data table is for 3CLpro, where cell G7 and G9 represent the two target formulations of PLGA-ICG-STR and PLGA-STR, respectively. The lower data table is for PLpro, with cells G3 and G5 representing the two target formulations of PLGA-ICG-Aloin and PLGA-Aloin, respectively. Cells A1, B1, and C1 serve as blanks for reference to act as positive controls, with complete

	1	2	3	4	5	6	7	8	9	10	11	12
A	3310	581	467	1229	824	3441	2927	3882	3729	3709	3518	3574
B	3223	595	470	1187	818	3357	2921	3784	3572	3520	3442	3487
C	3221	594	503	1218	799	3392	2859	3640	3548	3596	3383	3448
D	3542	3538	84	3711	1502	459	3688	3637	3570	3565	3395	3437
E	3527	3492	83	3580	1512	449	3593	3612	3636	3673	3534	3451
F	3459	3418	85	3537	1520	469	3554	3688	3636	3527	3493	3435
G	2992	1394	500	860	647	1438	623	1267	763	3053	1339	655
H	1099	527	3584	3776	3751	3881	221	201	222	108	99	103

	1	2	3	4	5	6	7	8	9	10	11	12
A	3398	507	449	1145	740	3661	2827	4092	3984	3994	3736	3138
B	3388	526	437	1134	729	3633	2780	3896	3821	3662	3752	3695
C	3384	526	444	1133	718	3540	2715	3853	3742	3742	3966	3729
D	3759	3810	88	3932	1589	486	3863	3829	3856	3619	3791	3748
E	3928	3829	87	3310	1569	517	3890	3775	3900	4086	3809	3674
F	3958	3842	88	3808	1563	508	3813	3835	3899	3588	3761	3696
G	3196	1054	545	792	492	3335	1100	822	1243	775	1088	769
H	1157	866	4170	4117	4063	4160	224	232	233	16	107	106

Figure 8. Assay results for 3CLpro (top) and PLpro (bottom).

fluorescence of the enzyme as it was able to catalyze its substrate in the absence of any drugs. In comparison with other drugs, the designed formulations showed their success, which indicates that the release of the compounds from the PLGA nanoparticles is successful, and there are likely no interactions between the drug and the nanoparticles themselves. Overall, this proves the success of these formulations *in vitro* and provides the data to proceed to *in vivo* testing in rats.

As a precursor to *in vivo* testing, cytotoxicity tests were done on the formulations to confirm they would not have any side effects that would result in adverse health conditions. The cytotoxicity assays used VERO C1008 cells, an epithelial cell line that closely resembles the epithelial cells in the human body. This specific cell line was chosen, as it is well established in the literature that the virus first infects the epithelial cells of the body, so testing the formulations to ensure they are not toxic to these cells is an accurate representation of its interaction with the bodily tissues of interest. The above image shows the cell line treated with the formulation underneath a microscope, where the cells can be seen as healthy and intact. The cytotoxicity results showed very little cell death, and after doing the calculations, it was determined there was no statistically significant relationship between the formulation and cell death, proving that the compounds were not cytotoxic. This provides the necessary basis for further testing and characterization *in vivo*.

3.3. Chemotaxis Models

Figure 9 indicates that the net chemotactic velocity is sufficient to move the nanoparticle towards the target cells based on a beta-actin concentration gradient. When there is very little beta-actin present, the net chemotactic velocity is very high according to the graph, and as the concentration begins to increase, the net velocity decreases, until it stabilizes at a value of approximately 50,000 nanometers per second squared. These calculations align correctly with the literature regarding chemotaxis; as substrate concentration increases, there are less available

active sites and therefore fewer free enzymes, since there is more substrate in the active sites of the enzymes. Only free enzymes chemotax, so as the number of free enzymes decreases, the net chemotactic velocity does too. However, seeing as the velocity stabilizes at 50,000 nanometers per squared second, it indicates that PKC-Delta is a viable nanomotor to use for this drug delivery system, as 50,000 nanometers squared per second is fairly significant in terms of drug delivery and should enable the nanoparticles to reach their target quickly and be in close proximity to it, increasing its effectiveness and inhibiting viral replication.

In Figure 10, the computationally calculated mean displacement line is in red, while the theoretical mean displacement is indicated by the dashed black line. The blue lines represent the displacement of each individual particle. Overall, when analyzing the mean displacement of the particles, which was calculated to be 44,721 nm, the chemotactic velocity is able to outpace Brownian diffusion by a factor of 9.62, further supporting the conclusion that PKC-Delta will be able to successfully transport the PLGA nanoparticles directly to viral cells in order to optimize the drug delivery system and have higher rates of viral inhibition.

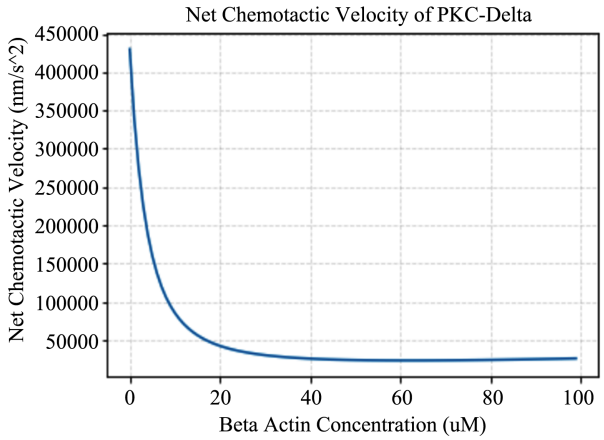

Figure 9. Graph of the new Chemotactic velocity of PKC-delta.

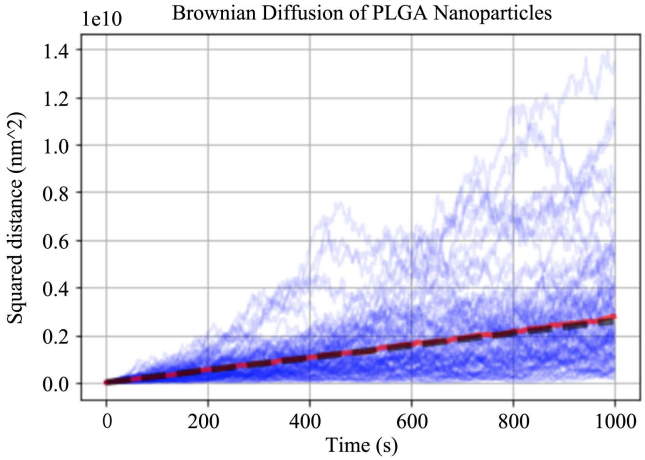

Figure 10. Graph of the mean displacement of PLGA Nanoparticles as a result of brownian diffusion.

4. Conclusions

Ultimately, this project served as the basis for a potential inhaled drug delivery system that utilized the phenomenon of enzyme chemotaxis as a way to target the nanoparticles specifically towards the viral cells. This enabled higher quality of treatment, as the delivery of the drug will be site-specific and in close proximity to the viral cell itself, meaning that a higher concentration of the drug will be present to inhibit the viral replication of SARS-COV-2. The work done in this project identified two potential therapeutics that have shown *in vitro* success in inhibiting the replication of SARS-COV-2, as well as the synthesis of nanoparticles with those therapeutics encapsulated that can be tested *in vivo*. Finally, computational modeling of the enzyme kinetics of PKC-Delta and its opposing force proved that PKC-Delta can sufficiently overcome the opposing force of Brownian diffusion and serve as a viable enzyme nanomotor to propel this drug delivery system.

However, there are some limitations that this project needs to address moving forward. For instance, the release profile of the drugs encapsulated in PLGA has not yet been identified, and it must be proven that there is no chemical interaction/binding between the drug and the vesicle. Using differential scanning calorimetry and thermogravimetric analysis, both these claims can be proven to further the validity of this drug delivery system as a potential treatment to Covid-19. Furthermore, the current model for the enzyme kinetics of PKC-Delta lacks pharmacokinetic parameters, which may cause a discrepancy between the *in silico* and *in vivo* data, as the characterization of PKC-Delta required some parameters and constants that had not yet been experimentally verified in the literature. Fortunately, approval for *in vivo* testing of this system in rats has already been acquired, so moving forward, this system can be further explored and characterized as a potential method to inhibit viral replication of Covid-19, severely decreasing its severity in patients and reducing transmission to other hosts, which would help bring an end to this global pandemic. Finally, Covid-19 is not entirely within the lungs, as it spreads to other organs as well. This treatment targets early stage Covid-19, when it is only within the lungs, but modifications must be made to account for other organs.

Future considerations aim to gather further data on the validity of this formulation as a method to treat Covid-19, as the current success has only been proven *in vitro*. In addition to *in vivo* testing, the laboratory is working with a pharmaceutical company in the United Kingdom to whom these formulations are being shipped in order to see viral testing. The laboratory does not have the clearance to directly work with the virus; only the enzymes from the virus, so this enables the collection of further *in vitro* data that is specific to the virus itself. Furthermore, this research received validation from several professors and fellows at a national conference of the American Chemical Society, and is currently on the path to being published in a peer-reviewed journal. Finally, the laboratory is currently pending a patent for the novel synthesis of these novel nanoparticles,

alongside other compounds, in order to distribute this formulation to as many people as possible when all approvals have been acquired. Overall, this project designs an end-to-end drug delivery system that can be easily deployed to save hundreds of thousands of lives.

Acknowledgments

I would like to thank Dr. Vicky Mody and Dr. Darrel Velegol for providing assistance and resources that made this project possible.

Conflicts of Interest

The author declares no conflicts of interest regarding the publication of this paper.

References

[1] Johns Hopkins Coronavirus Resource Center. Covid-19 Map. https://coronavirus.jhu.edu/map.html

[2] Shang, J., Wan, Y.S., *et al.* (2020) Cell Entry Mechanisms of SARS-COV-2. *PNAS*, **117**, 11727-11734. https://www.pnas.org/content/117/21/11727#ref-3

[3] Centers for Disease Control and Prevention, Centers for Disease Control and Prevention (2019) Vaccine Breakthrough Infections: The Possibility of Getting COVID-19 after Getting Vaccinated. https://www.cdc.gov/coronavirus/2019-ncov/vaccines/effectiveness/

[4] Rajpoot, S., *et al.* (2020) Dual Targeting of 3CLpro and PLpro of SARS-COV-2: A Novel Structure-Based Design Approach to Treat COVID-19. *Current Research in Structural Biology*, **3**, 9-18. https://www.sciencedirect.com/science/article/pii/S2665928X20300258

[5] National Institute of Biomedical Imaging and Bioengineering and U.S. Department of Health and Human Services. Drug Delivery Systems. https://www.nibib.nih.gov/science-education/science-topics/drug-delivery-systems

[6] Somasundar, A., *et al.* (2019) Positive and Negative Chemotaxis of Enzyme-Coated Liposome Motors. *Nature Nanotechnology*, **14**, 1129-1134. https://www.nature.com/articles/s41565-019-0578-8

[7] Falk, M.D., Liu, W., *et al.* (2014) Enzyme Kinetics and Distinct Modulation of the Protein Kinase N Family of Kinases by Lipid Activators and Small Molecule Inhibitors. *Bioscience Reports*, **34**, e00097. https://www.ncbi.nlm.nih.gov/pmc/articles/PMC3958129/